Computer Vision Applications for the Gemini Planet Imager

Dmitry Savransky and Lisa Poyneer

Lawrence Livermore National Laboratory

May 22, 2013

This work performed under the auspices of the U.S. Department of Energy by Lawrence Livermore National Laboratory under Contract DE-AC52-07NA27344. LLNL-PRES-636972

Motivation

Retrieved from `http://exoplanetarchive.ipac.caltech.edu` on 03.28.13

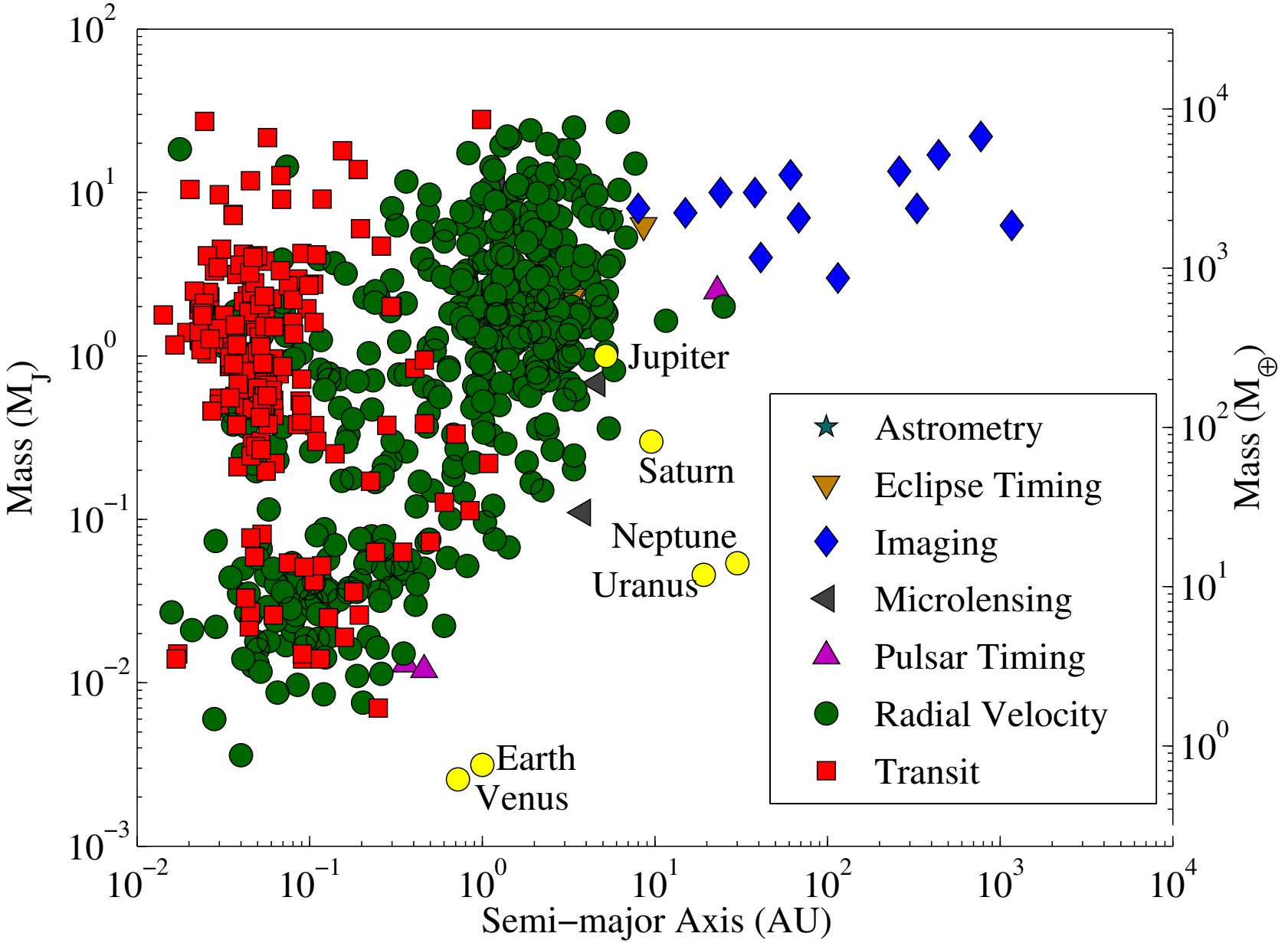

Planets are much much fainter than stars...

The brightest planets are still one million times fainter than their host stars

Commercial CCDs can achieve contrasts of 2048:1
The human eye can achieve 16384:1

...So we block the star

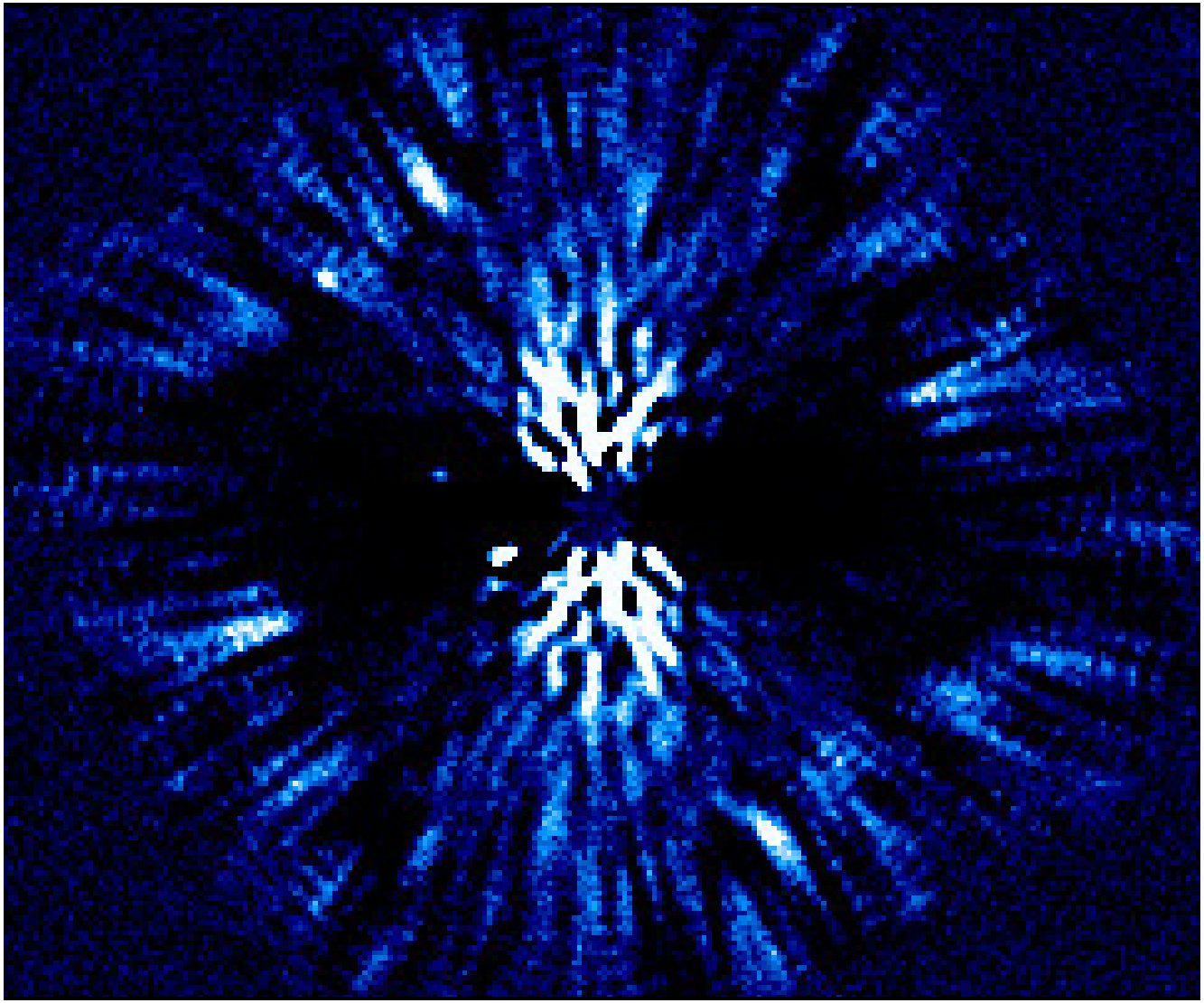

Figure: Simulated, post-processed GPI data set.

The Gemini Planet Imager

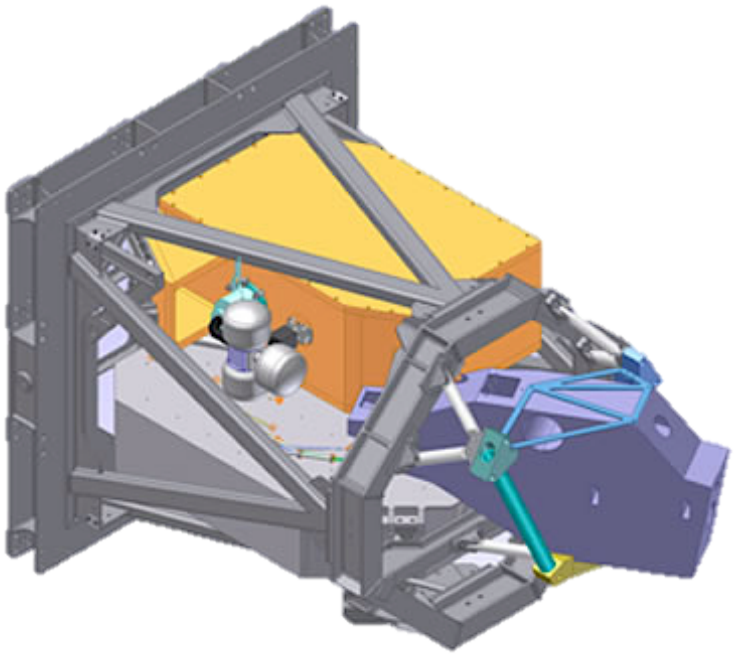

GPI Model.

GPI as-built.

The Gemini Planet Imager

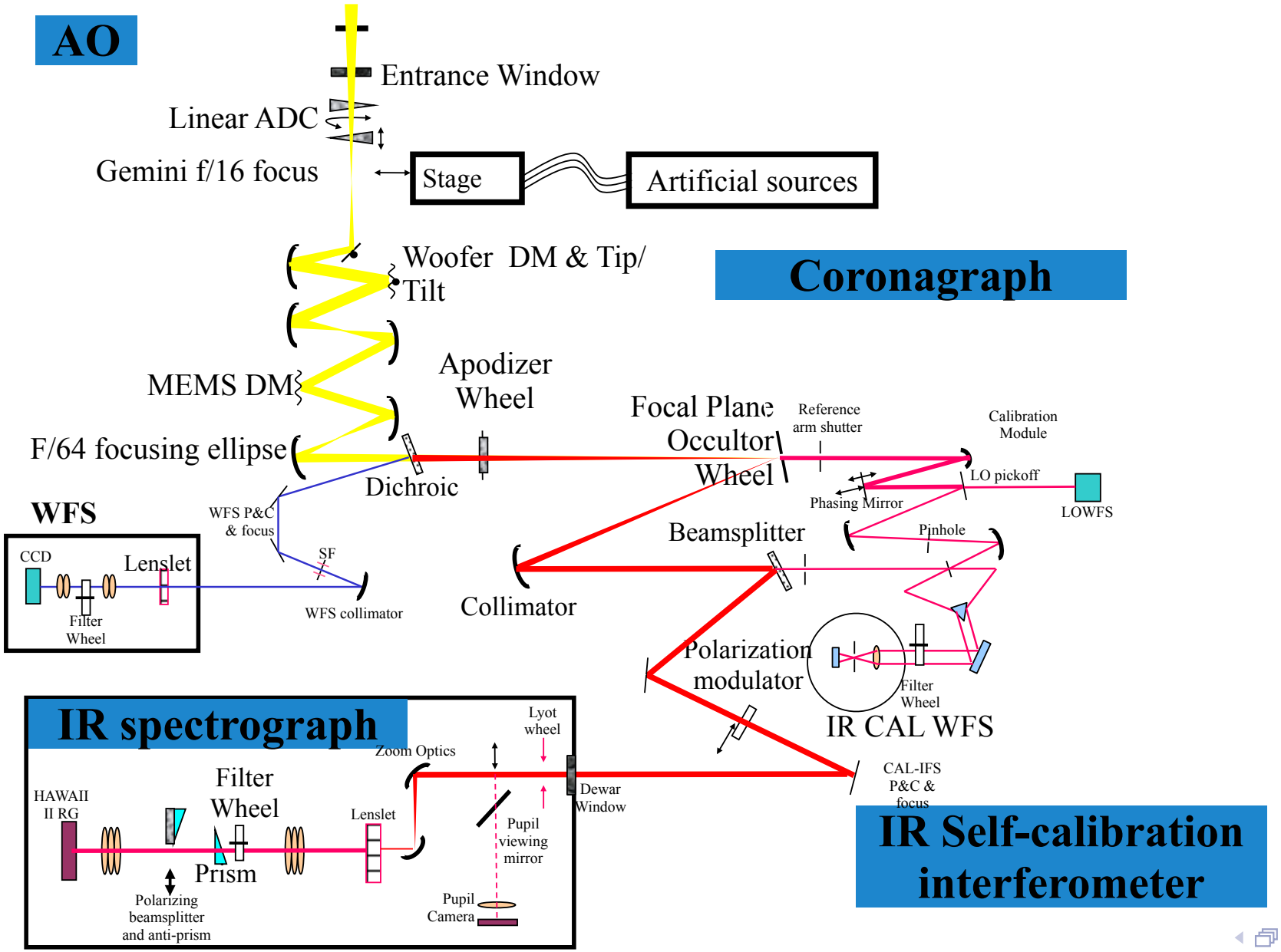

Lyot Coronagraphy

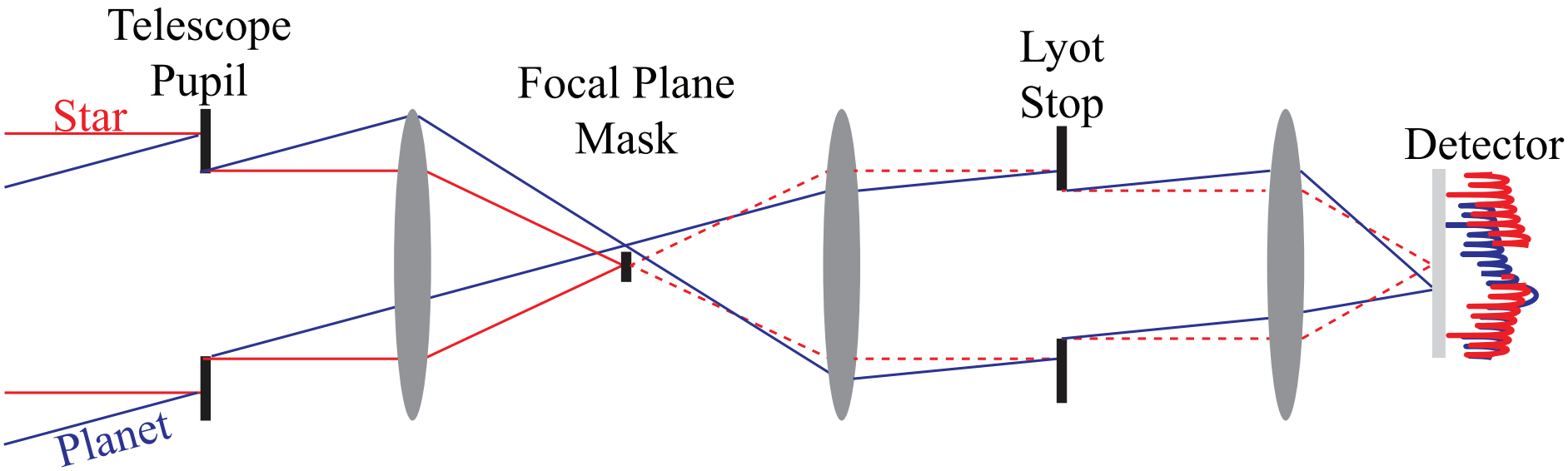

Figure: Lyot coronagraph. Based on [Sivaramakrishnan et al., 2001].

Lyot Coronagraphy

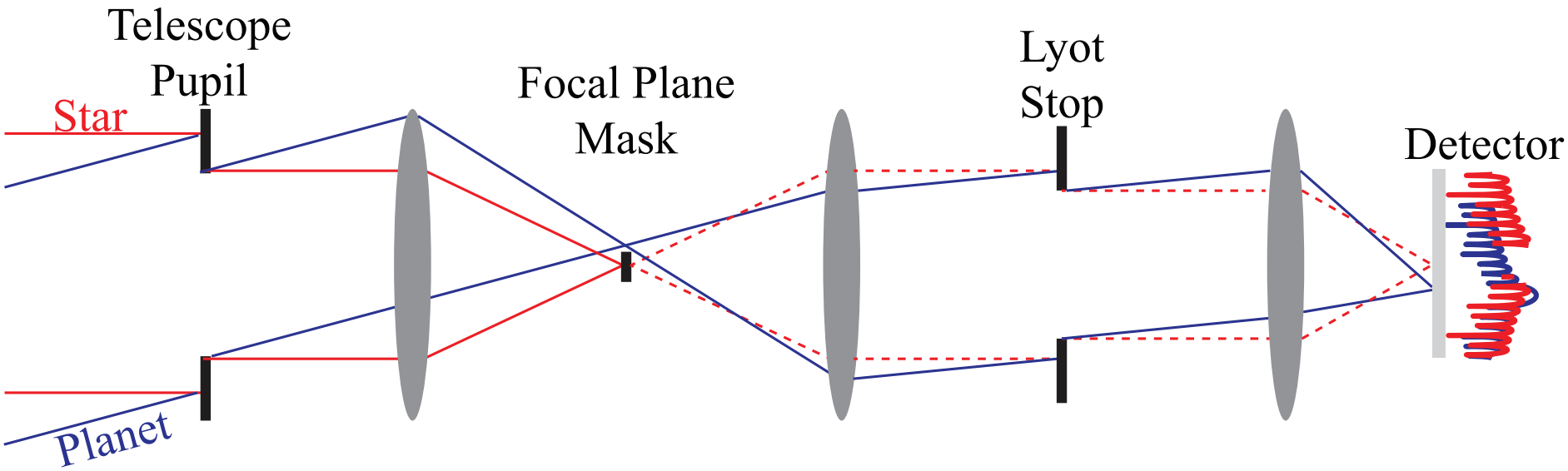

Figure: Lyot coronagraph. Based on [Sivaramakrishnan et al., 2001].

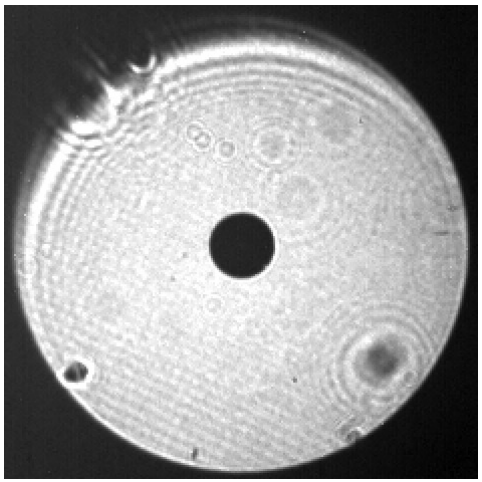

Pupil

Lyot Coronagraphy

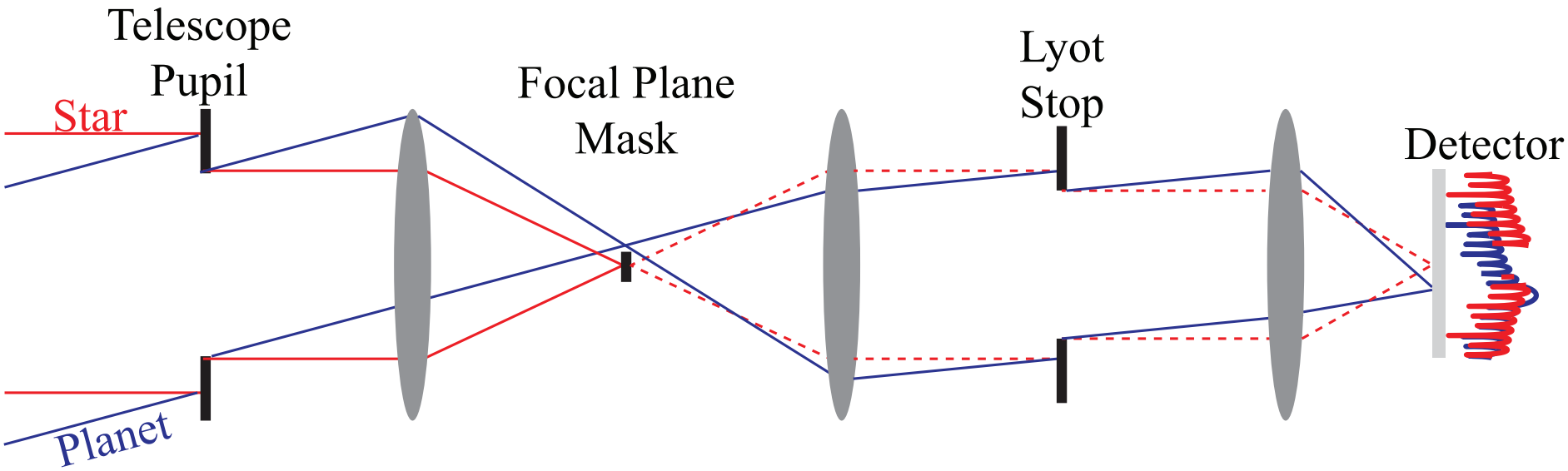

Figure: Lyot coronagraph. Based on [Sivaramakrishnan et al., 2001].

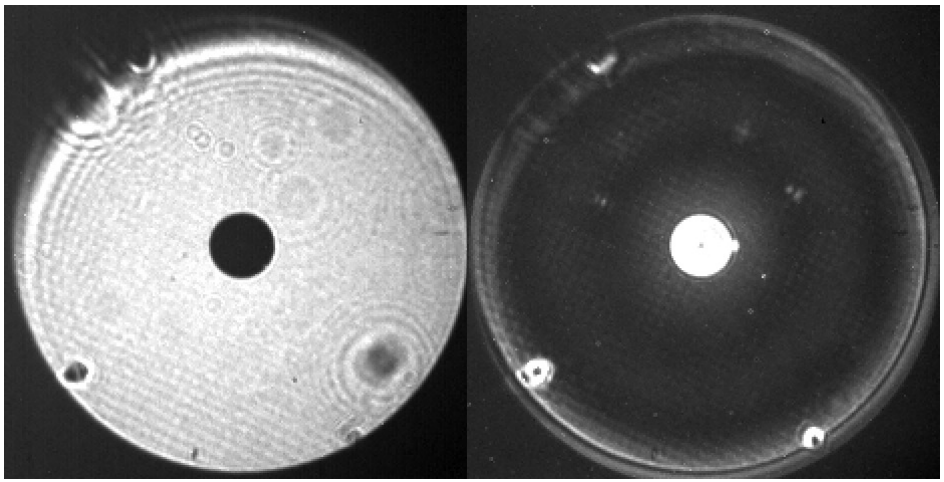

Pupil FPM

Lyot Coronagraphy

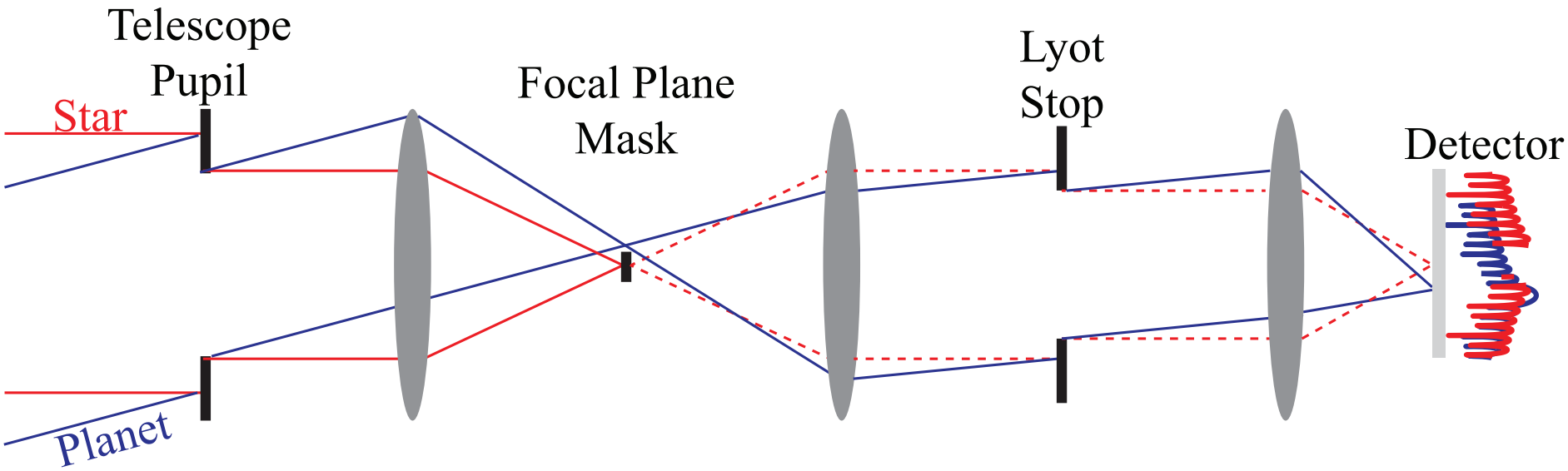

Figure: Lyot coronagraph. Based on [Sivaramakrishnan et al., 2001].

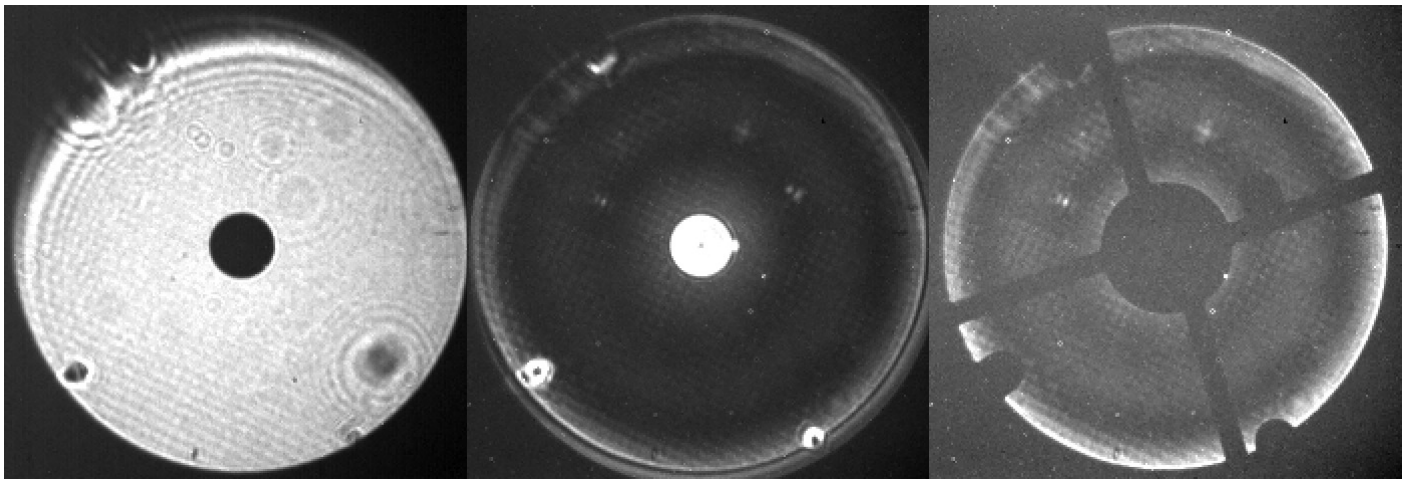

Pupil FPM FPM+Lyot

Lyot Coronagraphy

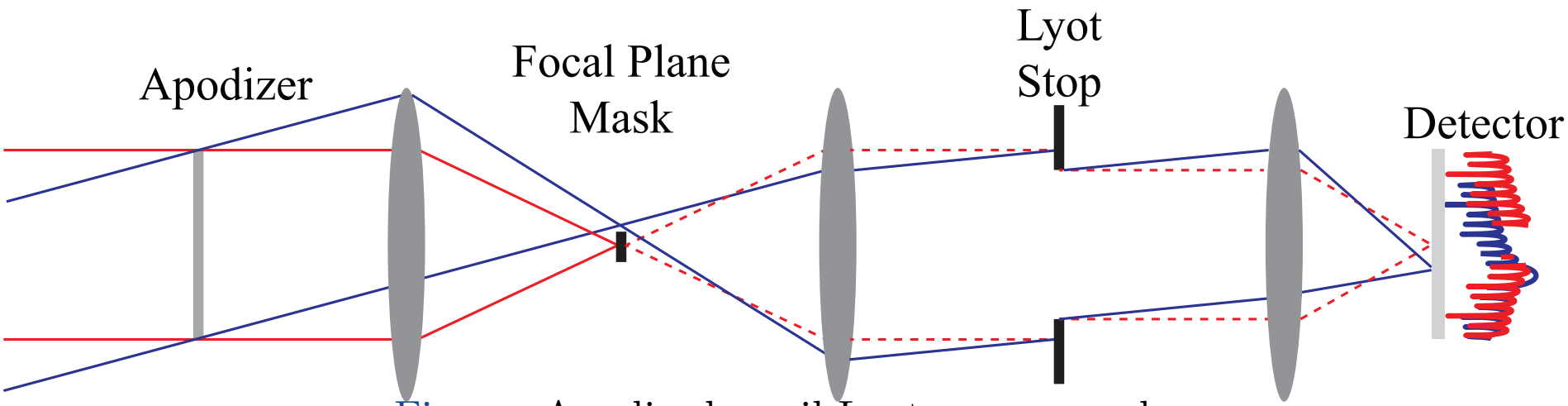

Figure: Apodized pupil Lyot coronagraph.

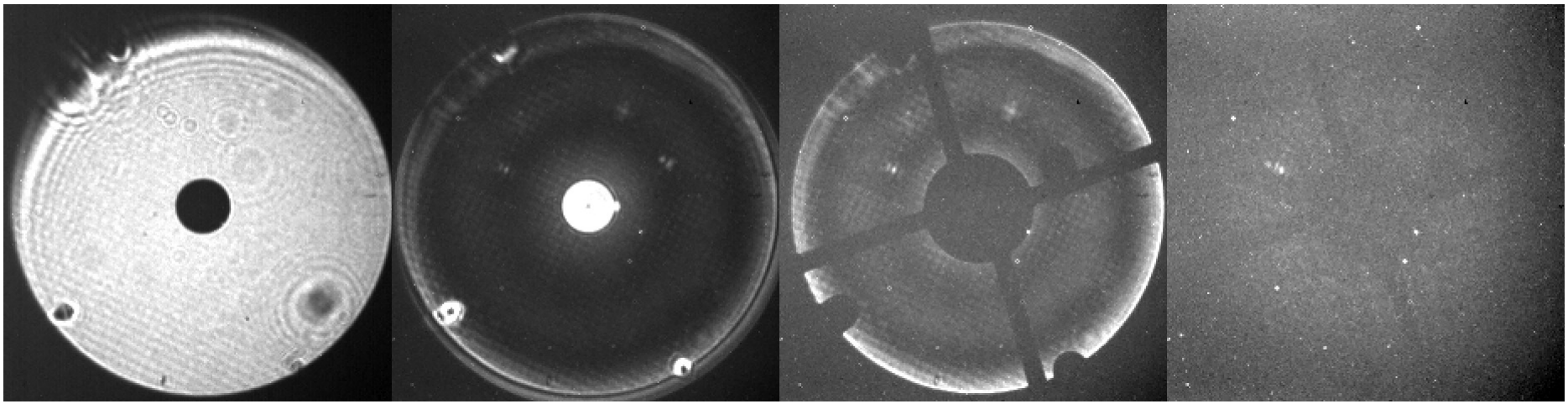

Pupil FPM FPM+Lyot Apodizer+FPM+Lyot

Apodized Pupil Lyot Coronagraphy

Pre-apodize to remove residual diffraction:

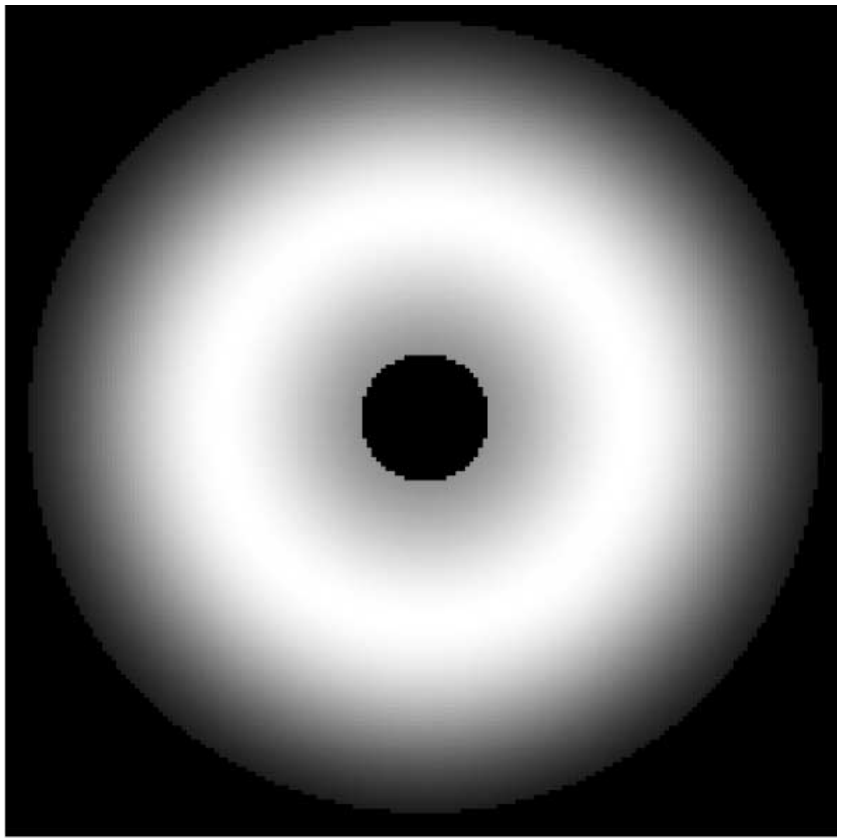

Apodizer function

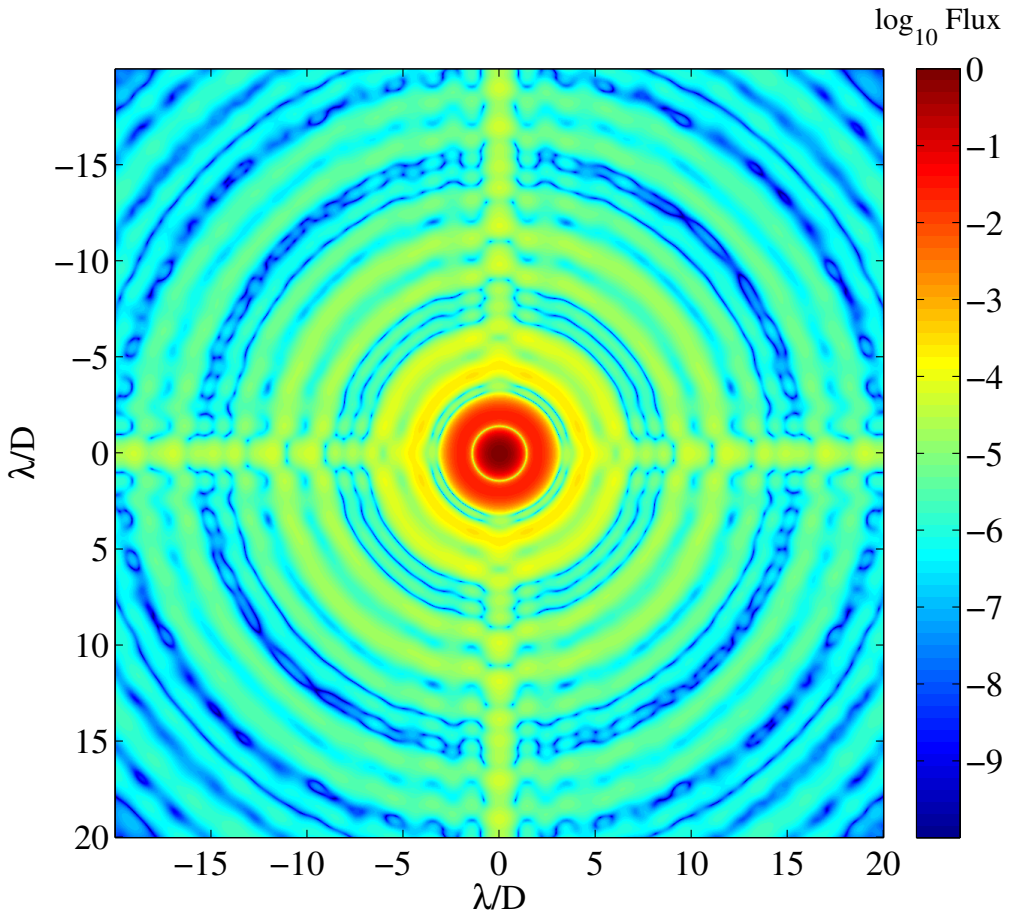

Point Spread Function

See: "Apodized Pupil Lyot Coronagraphs for Arbitrary Telescope Apertures" [Soummer, 2005]

System Alignment

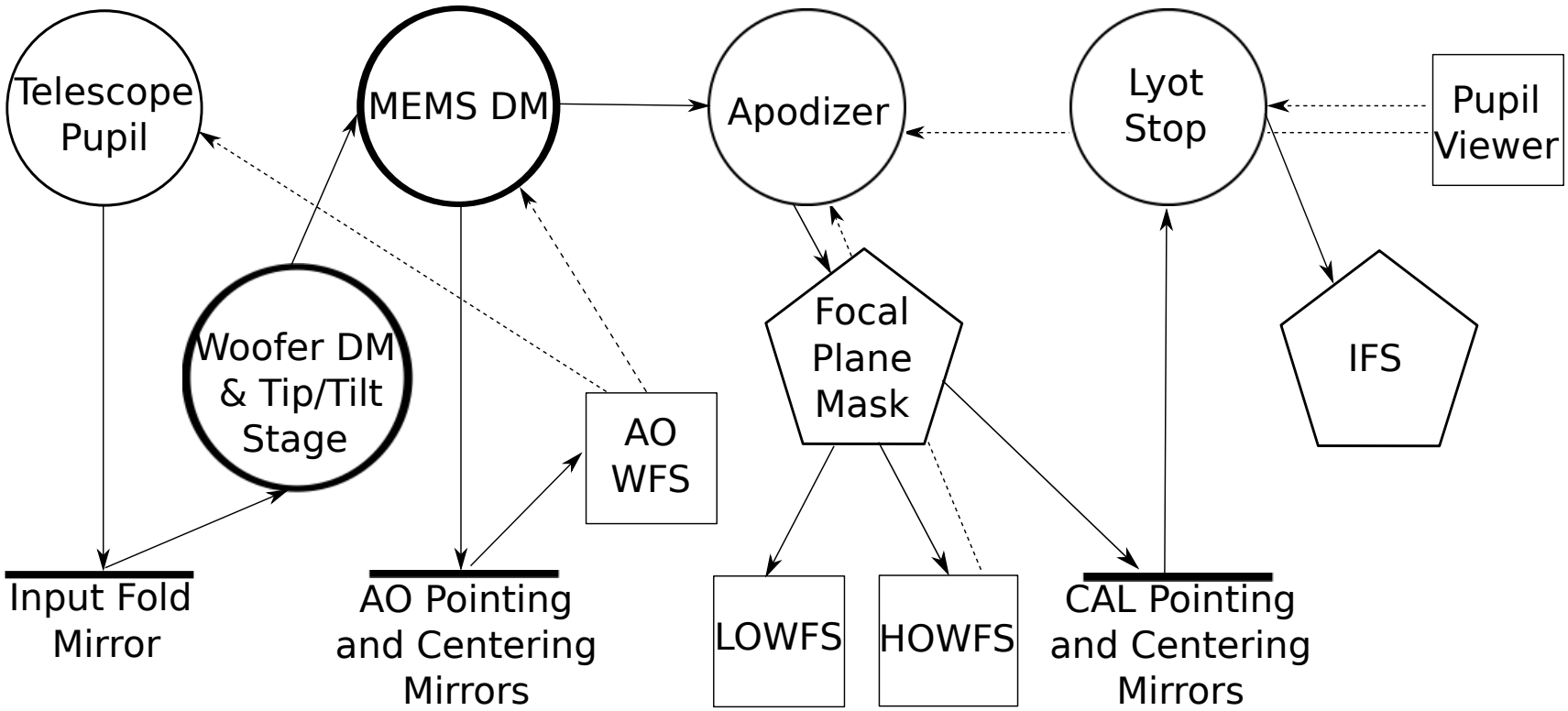

Figure: Apodizer and Lyot Stop must be aligned to MEMS DM to within 0.5% and 1% of their pupil sizes, respectively.

Finding Pupil Centers - Elliptical Hough Transform

[Ballard, 1981, Xie and Ji, 2002]

- Want to extract regular features (ellipses) formed by the central obscurations of apodizers and Lyot stops
- Use a generalized Hough transform with ellipse shape class:

$$\frac{(x-x_0)^2}{a^2} + \frac{(y-y_0)^2}{b^2} = 1$$

- Define candidate pixels based on intensity variations
- Define accumulator array for the semi-minor axis

$$b = \sqrt{\frac{a^2\left[(2ad)^2 - (a^2+d^2-f^2)^2\right]}{a^4 - (a^2+d^2-f^2)^2}}$$

$$d \triangleq \sqrt{(x_p - x_0)^2 + (y_p - y_0)^2}$$

$$f \triangleq \sqrt{(x_p - x_2)^2 + (y_p - y_2)^2}$$

Finding Pupil Centers

[Savransky et al., 2013]

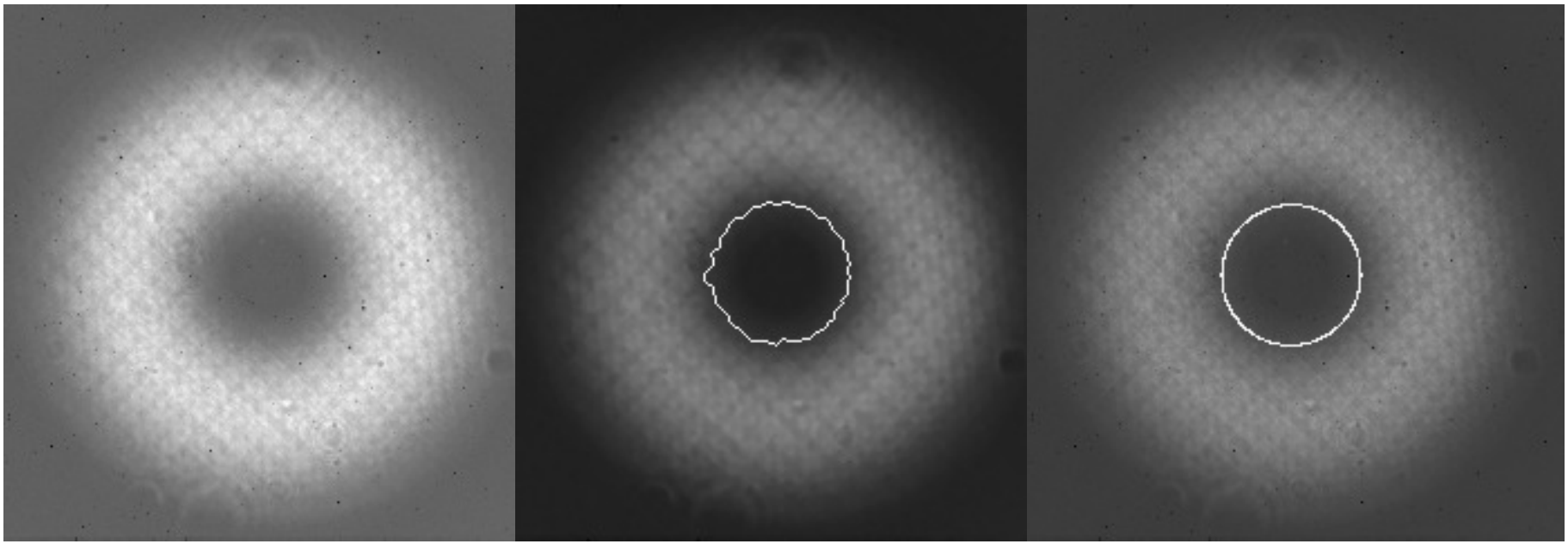

Figure: Pupil viewer images of the apodizer only (no FPM or Lyot stop in light path). *Left*: Dark subtracted pupil viewer image. *Center*: Median filtered image with the candidate pixels for the inner annulus of the apodizer overlaid. *Right*: Original image with best solution from Hough transform overlaid.

Aligning to the MEMS Plane

[Savransky et al., 2013]

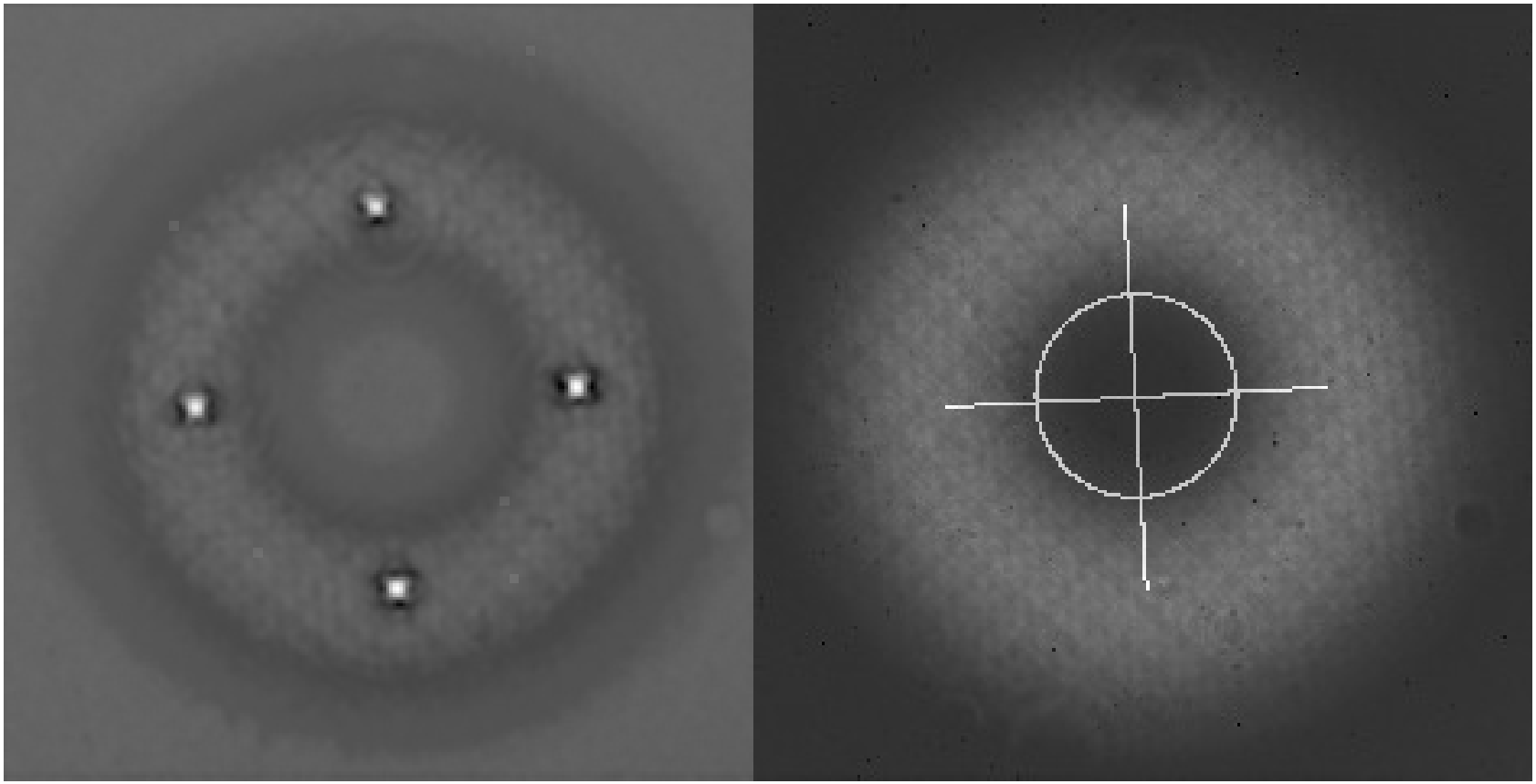

Figure: *Left*: Difference image between poked and flat DM states. *Right*: Original image with best solution from Hough transform and intersection of MEMS pokes overlaid.

Finding Geometric Shapes

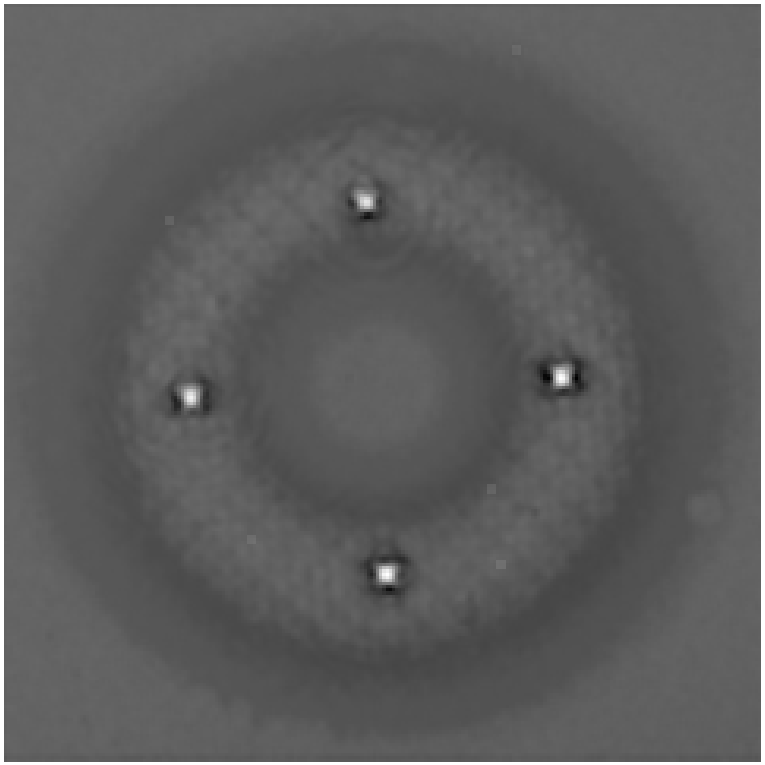

DM pokes on pupil viewer

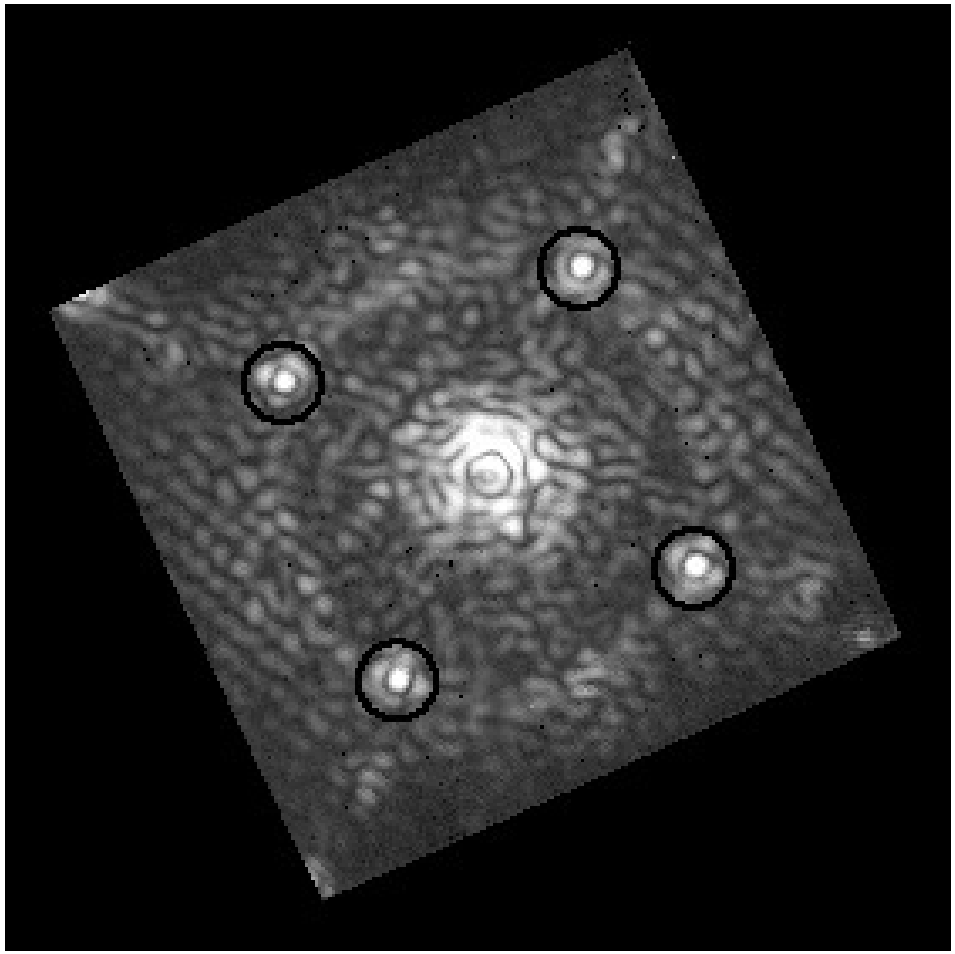

Astrometric calibration spots in IFS image

Finding Squares

- Assumptions:
  - Four points in the image are in the shape of a perfect square
  - Points are not the brightest but not the dimmest in the image
  - Square orientation is arbitrary with respect to image axes
  - Square size is arbitrary
- Procedure:
  - Select & remove brightest point in image
  - Test against all other candidate points, looking for squares:

$$\{d_k\}_{k=1}^{6} = \{\|\mathbf{r}_i - \mathbf{r}_j\| : i, j \in \{{}_4C_2\}\}$$

$$d_1 = d_2 = d_3 = d_4 = d_5/\sqrt{2} = d_6/\sqrt{2}$$

- Breadth-first search over candidate points - grows by $(n+1)/(n-3)$ for each new point.

Finding Squares (Better)

- What if we could prune the tree as we search it?
- Every square contains a right triangle:

$$\{d'_k\}_{k=1}^{3} = \{\|\mathbf{r}_i - \mathbf{r}_j\| : i, j \in \{{}_3C_2\}\}$$

$$d'_1 = d'_2 = d'_3/\sqrt{2}$$

- Maintain sublist of candidates forming right triangles
- Test new candidates against sublist rather than against all candidates

Finding Squares In Action

[Savransky et al., 2013]

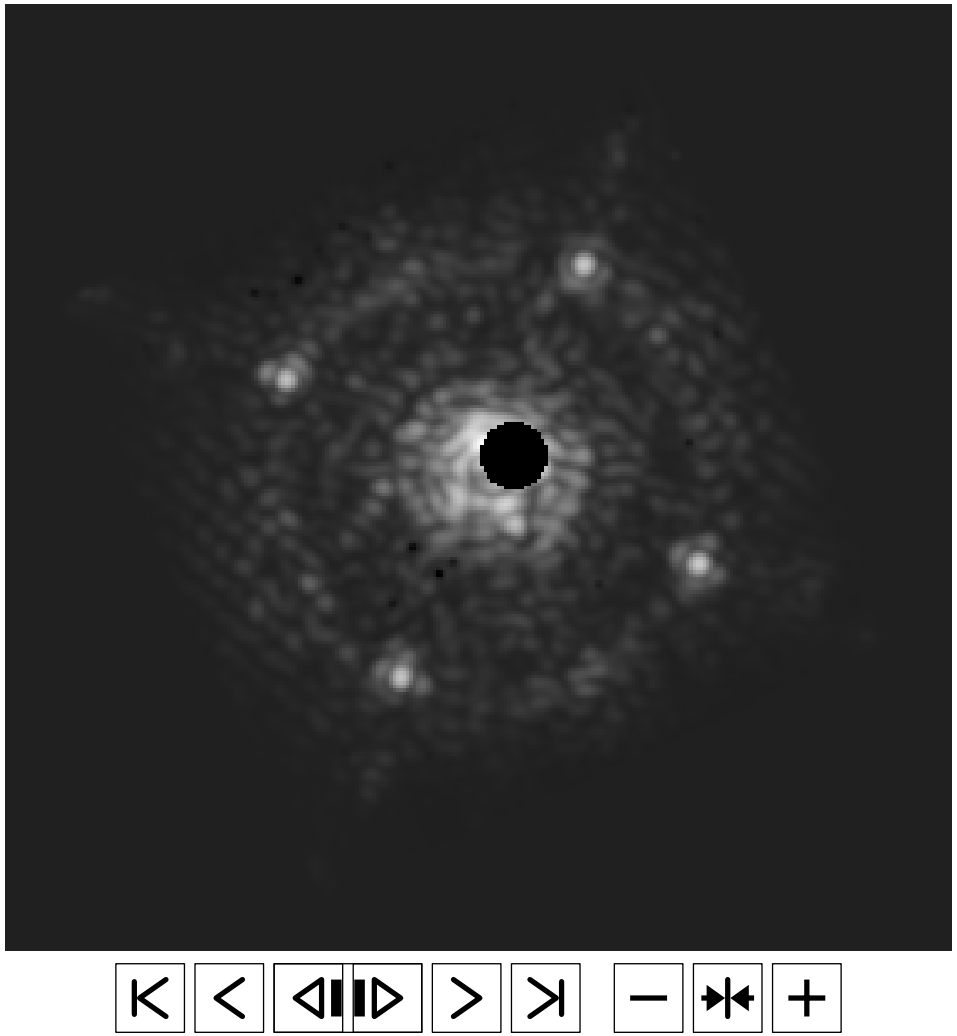

Finding Squares In Action

[Savransky et al., 2013]

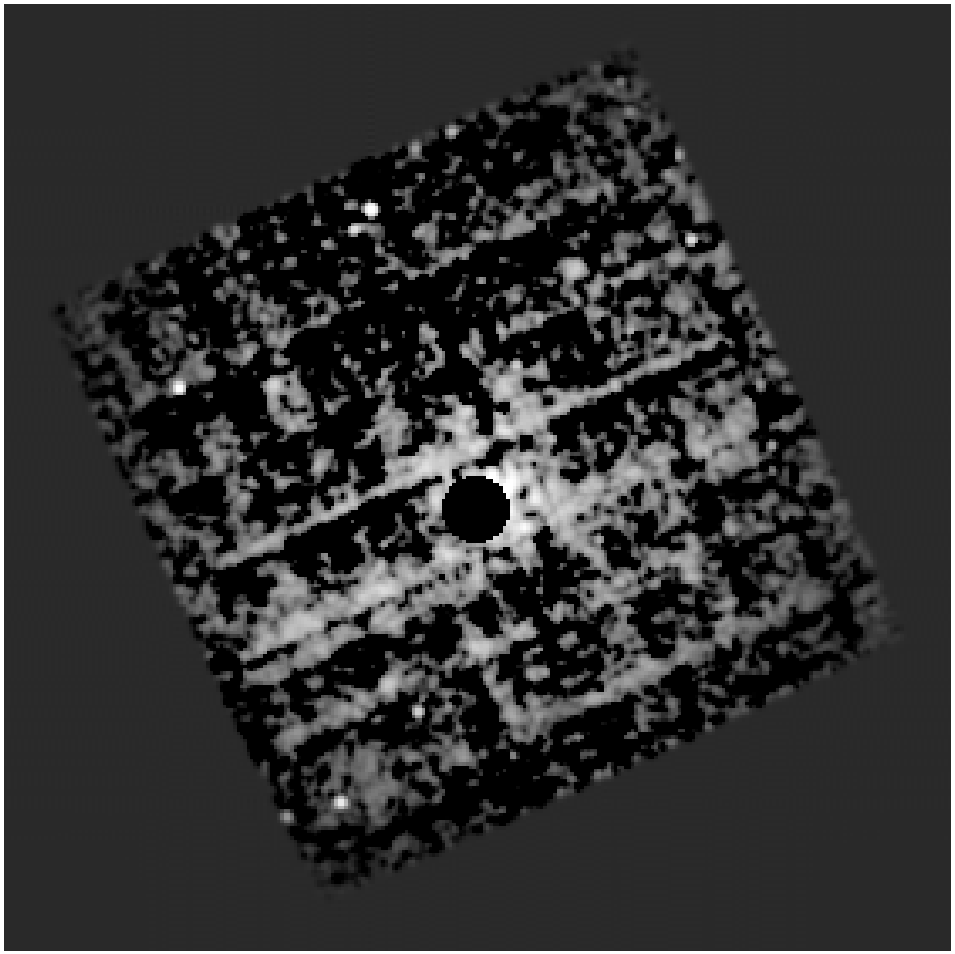

- Final satellite spot was added to candidate list on the 38th iteration
- 73815 possible combinations of four spots, or 7770 possible combinations of three spots from previous iteration
- Only 28 subsets (0.36%) had been identified as possible candidates for testing
- Total execution time was only 1.45 times longer than in previous case

Conclusions

- High-performance optical systems will continuously become more automated with stricter alignment tolerances and error budgets
- Simple techniques from machine learning and computer vision can be enormously helpful in automating basic alignment tasks and ensuring high repeatability
- Algorithms presented here are easy to code, and execute well on normal hardware
- Geometric feature identification is applicable to a variety of optical and laser systems and tasks

References I

Ballard, D. H. (1981).

Generalizing the hough transform to detect arbitrary shapes.
Pattern recognition, 13(2):111–122.

Savransky, D., Thomas, S. J., Poyneer, L. A., and Macintosh, B. A. (2013).

Computer vision applications for coronagraphic optical alignment and image processing.
Applied Optics, 52(14):3394–3403.

Sivaramakrishnan, A., Koresko, C. D., Makidon, R. B., Berkefeld, T., and Kuchner, M. J. (2001).

Ground-based coronagraphy with high-order adaptive optics.
The astrophysical journal, 552(1):397.

Soummer, R. (2005).

Apodized pupil lyot coronagraphs for arbitrary telescope apertures.
The Astrophysical Journal Letters, 618(2):L161–L164.

Xie, Y. and Ji, Q. (2002).

A new efficient ellipse detection method.
In *Pattern Recognition, 2002. Proceedings. 16th International Conference on*, volume 2, pages 957–960. IEEE.